Proc. Natl. Acad. Sci. USA
Vol. 96, pp. 8522–8527, July 1999
Cell Biology

Hsl7p, a negative regulator of Ste20p protein kinase in the *Saccharomyces cerevisiae* filamentous growth-signaling pathway

ATSUSHI FUJITA*, AKIO TONOUCHI, TAKATOSHI HIROKO, FUMIKA INOSE, TAKEYUKI NAGASHIMA, RIKA SATOH, AND SHIGEKO TANAKA

National Institute of Bioscience and Human Technology, Agency of Industrial Science and Technology, 1-1 Higashi, Tsukuba 305-8566, Japan

Edited by Fred Sherman, University of Rochester School of Medicine and Dentistry, Rochester, NY, and approved May 20, 1999 (received for review January 11, 1999)

ABSTRACT **In the budding yeast, *Saccharomyces cerevisiae*, protein kinases Ste20p (p21$^{Cdc42p/Rac}$-activated kinase), Ste11p [mitogen-activated protein kinase (MAPK) kinase kinase], Ste7p (MAPK kinase), Fus3p, and Kss1p (MAPKs) are utilized for haploid mating, invasive growth, and diploid filamentous growth. Members of the highly conserved Ste20p/p65^{PAK} protein kinase family regulate MAPK signal transduction pathways from yeast to man. We describe here a potent negative regulator of Ste20p in the yeast filamentous growth-signaling pathway. We identified a mutant, *hsl7*, that exhibits filamentous growth on rich medium. Hsl7p belongs to a highly conserved protein family in eukaryotes. Hsl7p associates with the noncatalytic region within the amino-terminal half of Ste20p as well as Cdc42p. Deletions of *HSL7* in haploid and diploid strains led to cell elongation and enhancement of both haploid invasive growth and diploid pseudohyphal growth. However, deletions of *STE20* in haploid and diploid greatly diminished these *hsl7*-associated phenotypes. In addition, overexpression of *HSL7* inhibited pseudohyphal growth. Thus, Hsl7p may inhibit the activity of Ste20p in the *S. cerevisiae* filamentous growth-signaling pathway. Our genetic analyses suggest the possibility that Cdc42p and Hsl7p compete for binding to Ste20p for pseudohyphal development when starved for nitrogen.**

The mitogen-activated protein kinase (MAPK) cascade is critical for various developmental events in eukaryotes (1–4). Elements of yeast single-MAPK pathway, Ste11p [MAPK kinase (MAPKK)], Ste7p [MAPK kinase kinase (MAPKK)], Kss1p, and Fus3p (MAPKs), are utilized for haploid mating, invasive growth, and diploid filamentous growth (5–9). Ste20p from *Saccharomyces cerevisiae* is a member of Ste20p/p65^{PAK} family of proteins kinases, which regulate conserved MAPK pathways (10–13). Ste20p also functions in several signal transduction pathways, including those involved in haploid mating (14), invasive growth (8), and diploid filamentous growth (5, 15).

In response to nitrogen limitation, diploid yeast cells undergo a dimorphic transition known as pseudohyphal differentiation (15). A dominant-activated form of Ras2p, the yeast homologue of mammalian Ras, causes enhanced pseudohyphal growth (15), and this effect is blocked by the dominant-negative form of Cdc42p, placing Cdc42p downstream of Ras2p (18). Cdc42p binds to the noncatalytic region within the amino-terminal half of Ste20p (19, 20). Interestingly, the interaction of Cdc42p with Ste20p, which is essential for proper localization of Ste20p, is required for haploid invasive growth and diploid pseudohyphal development, but not for pheromone response (19, 20).

Here we describe the identification of Hsl7p, a potent negative regulator of Ste20p in yeast filamentous growth-signaling pathway. Hsl7p is a member of highly conserved protein family ranging from yeast to man. Biochemical and two-hybrid analyses revealed that Hsl7p interacts with the amino-terminal half of Ste20p. Using a genetic approach, we show that Hsl7p may negatively regulate pseudohyphal development by modulating the binding of Cdc42p to Ste20p.

MATERIALS AND METHODS

Media, Growth, and Yeast Strains. Standard growth media and procedures for genetic manipulation of yeast have been described in detail (21). Synthetic low-ammonia medium (SLAD) for pseudohyphal development contains 50 μM ammonium sulfate, 2% glucose and 2% Bacto-agar (15). *S. cerevisiae* strains used in this study were YAF1151 (*MAT*α *his3 leu2 trp1 ura3 sir4*Δ::*HIS3 ace2*), YAF1108 (*MAT***a** *leu2 ura3*), YAF1110 (*MAT*α *leu2 ura3*), YAF1111 (*MAT***a**/*MAT*α *leu2/leu2 ura3/ura3*), YAF1191 (*MAT***a** *hsl7*Δ::*LEU2 leu2 ura3*), YAF1192 (*MAT***a** *ste20*Δ::*kan*^{r} *leu2 ura3*), YAF1193 (*MAT***a** *hsl7*Δ::*LEU2 ste20*Δ::*kan*^{r} *leu2 ura3*), YAF1194 (*MAT***a**/*MAT*α *hsl7*Δ::*LEU2/hsl7*Δ::*LEU2 leu2/leu2 ura3/ura3*), YAF1195 (*MAT***a**/*MAT*α *ste20*Δ::*kan*^{r}/*ste20*Δ::*kan*^{r} *leu2/leu2 ura3/ura3*), YAF1196 (*MAT***a**/*MAT*α *hsl7*Δ::*LEU2/hsl7*Δ::*LEU2 ste20*Δ::*kan*^{r}/*ste20*Δ::*kan*^{r} *leu2/leu2 ura3/ura3*), and YAF2009L (*MAT*α *his3 leu2 ura3*). All strains are derived from the Σ1278b genetic background except YAF1151. *HSL7*- and *STE20*-disrupted strains were constructed by using a one-step gene-disruption procedure (22). To construct the *HSL7*Δ::*LEU2* disruption plasmid, a 4.5-kb fragment encompassing *HSL7* was amplified by PCR and was cloned into pUC13 (pUC-HSL7). pUC-HSL7 was cleaved with *Eco*RV and *Eco*47III to remove the *HSL7* coding region. A *LEU2* fragment was ligated into the cleaved pUC-HSL7 to yield pUC-HSL7DL. To construct the *STE20*Δ::*kan*^{r} disruption plasmid, a 3.0-kb fragment encompassing *STE20* was amplified by PCR and was cloned into pUC13 (pUC-STE20). pUC-STE20 was cleaved with *Hpa*I to remove the *STE20* coding region. A *kan*^{r} *Pvu*II-*Eco*RV fragment from pUG6 (23) was ligated into the cleaved pUC-STE20 to yield pUC-STE20DK. pUC-HSL7DL and pUC-STE20DK were treated with *Eco*RI and were used for yeast transformations.

Screen for Mutants Exhibiting Filamentous Growth. The *Tn3-LEU2* transposon mutagenized yeast genomic library (24) was transformed into the strain YAF1151 (*MAT*α *his3 leu2 trp1 ura3 sir4*Δ::*HIS3 ace2*). Fifty thousand transformants were

The publication costs of this article were defrayed in part by page charge payment. This article must therefore be hereby marked "*advertisement*" in accordance with 18 U.S.C. §1734 solely to indicate this fact.

PNAS is available online at www.pnas.org.

This paper was submitted directly (Track II) to the *Proceedings* office. Abbreviations: MAPK, mitogen-activated protein kinase; MAPKK, MAPK kinase; MAPKKK, MAPKK kinase; PAK, p21$^{Cdc42p/Rac}$-activated kinase; GST, glutathione *S*-transferase; MBP, maltose-binding protein; SLAD, synthetic low-ammonia medium; AD, activation domain; LBD, LexA-binding domain; ori, origin of replication.

*To whom reprint requests should be addressed. e-mail: atsushi@nibh.go.jp.

plated on synthetic complete medium lacking leucine and were screened for filamentous growth by the observation of colony morphology and microscopic analysis. The yeast sequences adjacent to the *Tn3-LEU2* insertion were determined by using plasmid-rescue procedures (24). The yeast sequences were compared with those in the GenBank database by using the BLAST program (25).

Plasmids. To construct a fusion of glutathione *S*-transferase (GST) with full-length Ste20p, the *STE20* coding region was amplified by PCR and ligated into pGEX-2T (Pharmacia) to yield pGEX-STE20. pGEX-STE20$^{1-495}$ and pGEX-STE20$^{\Delta 258-842}$ carrying fusions of GST with the Ste20p$^{1-496}$ and Ste20p$^{\Delta 258-842}$ were constructed by removing an *Eco*RI fragment and a *Hin*dIII fragment of pGEX-STE20, respectively. pGEX-STE20$^{258-495}$ carrying a fusion of GST with Ste20p$^{258-495}$ was created by cloning an *Eco*RI-*Hin*dIII fragment of pUC-STE20 into pGEX-2T. To construct pMAL-P2-HSL7 carrying a fusion of maltose-binding protein (MBP) with full-length Hsl7p, a fragment including the *HSL7* coding region was amplified by PCR and ligated into pMAL-P2 (New England Biolabs).

Plasmid YEUp-HSL7 was constructed by cloning of *HSL7* into the high-copy vector YEUp3 (pUC13 + *URA3* + 2 μm ori). Plasmid YEUp-HSL7Lp was constructed by cloning a 1.0 kb fragment containing the promoter of *LEU2* into the *Nhe*I site of YEUp-HSL7 which corresponds to just upstream of *HSL7* ORF. Plasmid YCLp-CDC42 was constructed by cloning of a *Bgl*II-*Hin*dIII DNA fragment containing *CDC42* into the low-copy vector, pRS315 (pBluescript + *LEU2* + *CEN*/*ARS*) (26). YELp-STE20 was constructed by cloning of the DNA fragment containing *STE20* into the high-copy vector, pL1 (pUC19 + *LEU2* + 2 μm ori).

Resin-Binding Assay. GST-Ste20p and its deletion mutants expressed in the *Escherichia coli* strain MC1061 were purified on glutathione-Sepharose (Pharmacia) as described previously (27). Hsl7p tagged with MBP was purified by using the protease-deficient *E. coli* strain BL21. Cells of BL21 harboring pMAL-P2-HSL7 were grown at 37°C in LB. Expression of MBP-Hsl7p was induced by the addition of isopropyl β-D-thiogalactoside to a final concentration of 0.1 mM at OD_{600} = 0.4, followed by incubation at 37°C for 3 hr. Cells were harvested by centrifugation, resuspended in sonication buffer (20 mM Tris·HCl, pH 7.5/20 mM NaCl/50 mM EDTA/1 mM 2-mercaptoethanol/1% Triton X-100/1 mM PMSF/2 μg/ml leupeptin/2 μg/ml aprotinin), and disrupted by gentle sonication at 4°C. MBP-Hsl7p was purified by using amylose resin according to the manufacturer's protocol (New England Biolabs) except for elution; MBP-Hsl7p was eluted from the beads by elution buffer (50 mM Tris·HCl, pH 7.5/150 mM NaCl/1.5 mM $MgCl_2$/1 mM 2-mercaptoethanol/10 mM maltose). Ten micrograms of GST-Ste20p fusions were bound to 10 μl of glutathione-Sepharose beads in 200 μl of binding buffer (50 mM Tris·HCl/100 mM NaCl/5 mM $MgCl_2$/1 mM DTT/0.5 mg/ml BSA/0.07% Triton X-100) by incubating at 4°C for 1 hr. The beads were washed once with binding buffer, resuspended in binding buffer containing 10 μg of MBP-Hsl7p to a total volume of 200 μl, and then incubated at 4°C for 1 hr with gentle shaking. After incubation, the beads were washed five times with binding buffer and resuspended in 30 μl of Laemmli buffer (39). Proteins were separated by SDS/PAGE and transferred to poly(vinylidene difluoride) membranes. Blots were probed with antiserum against MBP (New England Biolabs), and then bound antibodies were detected by using alkaline phosphatase-coupled secondary antibody (Bio-Rad).

Assays for Invasive Growth, Filament Formation, and β-Galactosidase Activity. Assays for haploid invasive growth (8) and diploid pseudohyphal growth (5, 15) were performed as described. Plasmid YEpU-FTyZ (6), encoding the *lacZ* gene under the transcriptional control of filamentous response element (*FRE*) from Ty1 (28), was used for reporter assays. β-Galactosidase assays were performed with extracts from exponentially growing cells in synthetic dextrose (SD) medium at 30°C. For assays under nitrogen-starved conditions, extracts were prepared from the cells spread on SLAD medium plates for 3 days at 30°C. Cells always were washed with water before lysis. β-Galactosidase activities were normalized to the total protein in each extract by using a protein assay kit (Bio-Rad).

Two-Hybrid Analysis. Plasmids for two-hybrid analysis were constructed for this study. We constructed a vector (pAD1) for the expression of activation domain (AD) fusion by introducing the *HIS3* marker into the *Swa*I site of pYESTRP (Invitrogen) and a vector (pLBD1) for the expression of LexA-binding domain (LBD) fusion by introducing the *LEU2* marker into the *Ecl*136II site of pHybLex/Zeo (Invitrogen). pAD-Ste20pNH contains the N-terminal region of *STE20* (amino acids 1–495) fused to AD of pAD1. pLBD-Cdc42pL and pLBD-Hsl7pL contain full-length *CDC42* and *HSL7* fused to LBD of pLBD1, respectively. LBD-Cdc42p fusion incorporates the C188S substitution, which prevents prenylation. pLexAop-lucU is a luciferase reporter plasmid containing 8 LexA operator sites upstream of the luciferase gene on YEUp3 (pUC13 + *URA3* + 2 μm ori). pLexAop-LucU-Cdc42p contains *CDC42* on pLexAop-LucU. pLexAop-LucU-Hsl7p contains the *LEU2*-promoter-*HSL7* ORF fusion on pLexAop-LucU. Two-hybrid experiments were performed with strain YAF2009L (*MAT*α *his3 leu2 ura3*). The strain was transformed with an LBD plasmid, an AD plasmid, and a LexAop-luciferase reporter plasmid. Cells were grown to midlog phase in SD medium (21) and were assayed for luciferase activity with PicaGene assaying kit (Nippon Gene, Toyama, Japan). Each value represents the average for three independent cultures.

Microscopy. Yeast cells were photographed with a Leitz DMRD microscope with a ×40 objective lens. Colonies on plates were photographed with a Leica MZ APO microscope.

RESULTS

Identification of Mutants Exhibiting Filamentous Growth on Nitrogen-Rich Medium. To identify negative regulators of filamentous growth, we attempted to isolate mutants that exhibit filamentous growth on rich medium (not under the nitrogen-starved conditions). Pseudohyphal development under nitrogen-starved condition occurs only in *MAT***a**/*MAT*α diploid cells (15). However, recessive mutations are difficult to isolate by using *MAT***a**/*MAT*α diploid strains. Therefore, we used a haploid *sir4*$^-$ strain, YAF1151 (*MAT***a** *his3 leu2 trp1 ura3 sir4*::*HIS3 ace2*). The *sir4* mutation allows transcription of the silent mating-type loci *HMR***a** and *HML*α. Thus, some phenotypes of haploid *sir4* strains (bipolar budding pattern, sterility, and pseudohyphal growth under nitrogen-starved conditions) are similar to those of *MAT***a**/*MAT*α diploid strains because of simultaneous expression of both **a** and α information. Furthermore, because the *ace2* mutation causes a defect in cell separation (29), we can distinguish the transformants exhibiting filamentous growth by their colony morphologies: colonies exhibiting filamentous growth are highly rugged (30). Mutagenesis for isolating mutants exhibiting filamentous growth was performed by using the *Tn3-LEU2* transposon mutagenized yeast genomic library (24). Fifty thousand independent Leu$^+$ colonies were visually screened for filamentous growth, and two mutants were obtained. Genomic DNAs immediately adjacent to the *Tn3-LEU2* insertions were cloned and sequenced. In a BLAST search, these two mutants were found to have transposon insertions at 502389 and 503762 on chromosome II. Both insertion sites occurred within in the ORF YBR133c encoding Hsl7p (Fig. 1*A*), which had been identified as a negative regulator of Swe1p, an inhibitor of cyclin-dependent kinase known as Cdc28p (31). Hsl7p encodes a predicted protein of 828 aa (95,148 Da). As reported by other workers (31–33), the amino acid sequence of Hsl7p has

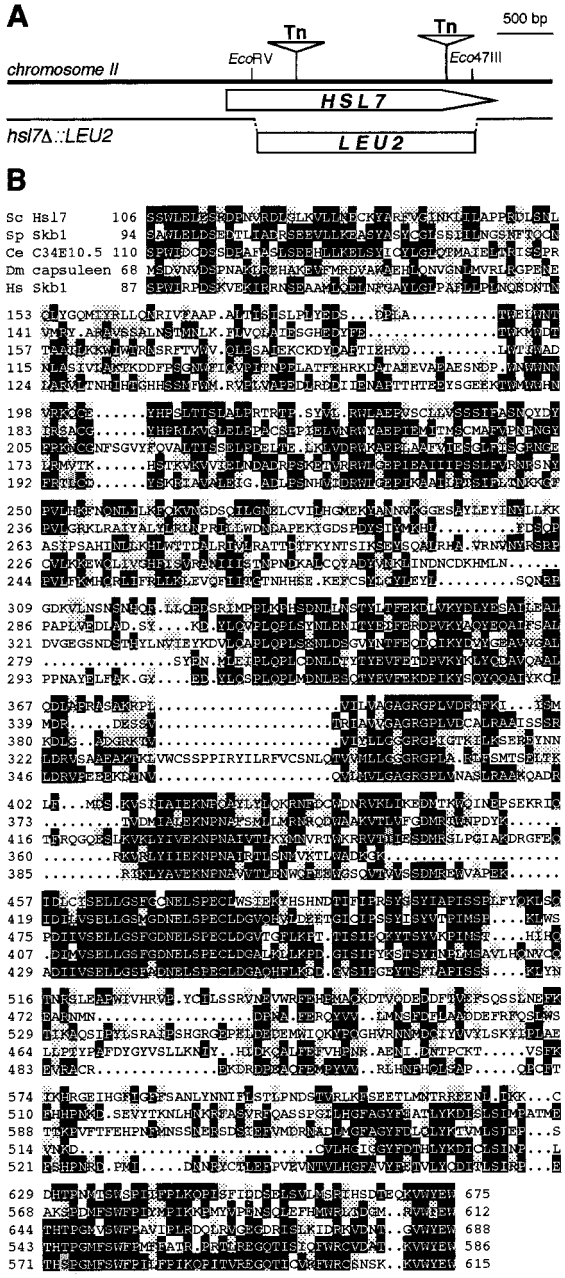

FIG. 1. (*A*) Restriction map of *HSL7*. Positions of *HSL7* ORF (open arrow) and the transposon insertion sites (triangles) are indicated. Structures of the fragment used to disrupt *HSL7* are noted. (*B*) Sequence alignment of *S. cerevisiae* Hsl7p with *S. pombe* Skb1p, *C. elegans* C34E10.5, *Drosophila* capsuleen, and human Skb1p proteins. Numbers indicate amino acid residue position. Identical and conserved residues are shown in white letters against black and shaded letters, respectively. GenBank accession nos.: Sc-Hsl7p, U65920; Sp-Skb1p, U59684; Ce-C34E10.5, U10402; Dm-capsuleen, AJ002740; Hs-Skb1p, AF015913.

sequence similarities with the amino acid sequences of *Schizosaccharomyces pombe* Skb1p, human Skb1p, and the *Caenorhabditis elegans* ORF C34E10.5 (Fig. 1*B*). Our BLAST search revealed the existence of a *Drosophila* homologue encoded by the *capsuleen* gene (Fig. 1*B*), thereby supporting the idea that Hsl7p/Skb1p/capsuleen protein family is conserved in eukaryotes.

Interaction of Hsl7p with Ste20p. *S. pombe* Skb1p is a protein that interacts with Shk1p [*S. pombe* Ste20p/p21$^{Cdc42p/Rac}$-activated kinase (PAK) homologue], as determined by using two-hybrid analyses (33, 34). *S. pombe* Shk1p is an essential component of the Ras- and Cdc42p-dependent signal transduction pathway required for cell viability, normal morphology, and sexual response. Skb1p may modulate Shk1p function in a signaling cascade to control morphology in *S. pombe* (33). Although biochemical interactions between Skb1p and Shk1p have not been detected (33), these results do suggest the possibility that Hsl7p interacts with Ste20p to regulate its function in *S. cerevisiae*. We used a resin-binding assay to examine the interaction of Hsl7p with Ste20p *in vitro*. We purified full-length Hsl7p as a fusion protein with MBP and full-length Ste20p as a fusion protein with GST. As shown in Fig. 2, MBP-Hsl7p bound to the full-length GST-Ste20p fusion, but not to GST alone. We next produced partial GST-Ste20p fusion proteins (Ste20p$^{1-495}$, Ste20p$^{258-495}$, and Ste20p$^{\Delta 258-842}$) (Fig. 2). Both GST-Ste20p$^{1-495}$ and GST-Ste20p$^{258-495}$ fusions bound to MBP-Hsl7p, but GST-Ste20p$^{\Delta 258-842}$ did not (Fig. 2). These results demonstrate that Hsl7p can bind to the noncatalytic region of Ste20p (amino acid 258–495) *in vitro*. Previous studies showed that the Rho-family GTPase Cdc42p binds to a conserved region (amino acid 335–370) in the noncatalytic N-terminal region of Ste20p (19, 20, 35) and that binding of Cdc42p with this region of Ste20p is essential for filamentous growth (19, 20). The identified Hsl7p-binding domain of Ste20p (amino acid 258–495) includes the Cdc42p-binding domain (amino acid 335–370).

We also used the two-hybrid system to confirm that Hsl7p can interact with the noncatalytic N-terminal region of Ste20p *in vivo*. *A HIS3*-based plasmid (pAD-Ste20pNH) was constructed to express the N-terminal region of Ste20p (amino acid 1–495) as a fusion to the C terminus of the B42 AD. *LEU2*-based plasmids (pLBD-Cdc42pL and pLBD-Hsl7pL) were constructed for expressing the full-length Cdc42p and Hsl7p as fusions to the C terminus of the LBD. An *S. cerevisiae* strain YAF2009L, which carries a plasmid (pLexAop-lucU) containing LexA-operator-luciferase reporter gene, was co-transformed with pLBD-Ste20pNH and pLBD-Cdc42pL or pLBD-Hsl7pL. Consistent with the previous observations, the

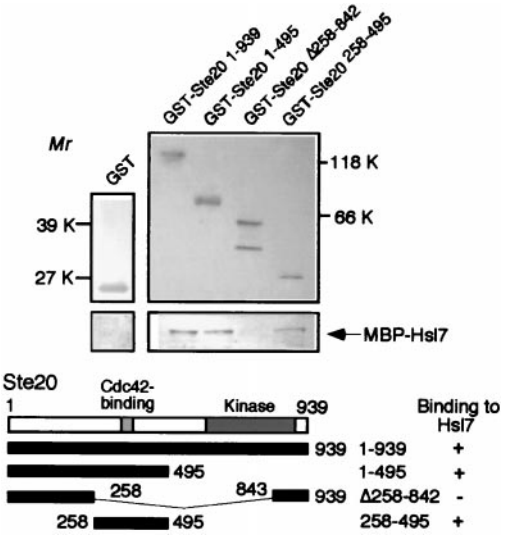

FIG. 2. Interaction of Hsl7p and Ste20p. Resin-binding assay was done to determine interactions between Hsl7p and Ste20p. GST fusion proteins with full-length Ste20p, Ste20p$^{1-495}$, Ste20p$^{258-495}$, and Ste20p$^{\Delta 258-842}$. GST were bound to glutathione-Sepharose beads and incubated with MBP-Hsl7p. After washing, proteins eluted with SDS-sample buffer were subjected to SDS/PAGE in 12.5% (upper left blot), 7.5% (upper right blot), and 5% (lower blots) gels and immunoblotted for the presence of GST, GST-Ste20p fusion proteins (upper blots), and MBP-Hsl7p (lower blots) with antibodies to GST (upper blots) and MBP (lower blots), respectively. Interactions between Ste20p fragments and Hsl7p are summarized at the bottom.

interaction of the N-terminal region of Ste20p with Cdc42p was detected (refs. 19 and 20; shown in Table 1). By two-hybrid analysis, we found weak interaction of Hsl7p with Ste20p (Table 1). Thus, biochemical and two-hybrid analyses demonstrated that Hsl7p can associate with the N-terminal region of Ste20p.

Genetic Evidence for Functional Interaction Between Hsl7p and Ste20p in Yeast Filamentous Growth-Signaling Pathway. To determine whether Hsl7p regulates the signaling cascade that controls haploid invasive growth and diploid pseudohyphal development by affecting the activity of Ste20p, strains deleted for *HSL7* (and/or *STE20*) were constructed. Because *HSL7* is not essential for growth (31), the *hsl7*Δ::*LEU2* fragment (Fig. 1*A*) was used to transform the wild-type *MAT***a** and *MATα* haploid strains. The resultant *MAT***a** and *MATα hsl7* disruptants were mated for the construction of *MAT***a**/*MATα hsl7*Δ/*hsl7*Δ homozygous diploid strains. Microscopic analysis revealed that the cells of both haploid and diploid *HSL7* disruptants are highly elongated (Fig. 3*A*). An elongated cell morphology of pseudohyphae is generated by hyperpolarized cell growth and delay of G_2/M cell cycle transition (36). Genetic study showed that Ste20p is essential for cell elongation (37). Disruption of *STE20* in both haploid *hsl7*Δ strains and diploid *hsl7*Δ/*hsl7*Δ strains exhibited normal, round shapes (Fig. 3*A*). Haploid strains grown on rich-medium plates exhibit invasive growth (8). Ste20p and elements of the MAPK cascade (Ste11p, Ste7p, Kss1p, and Fus3p) are also required for invasive growth (6–8). Deletion of *HSL7* resulted in greatly enhanced agar penetration (Fig. 3*B*), whereas the strain lacking both *HSL7* and *STE20* did not invade the agar (Fig. 3*B*). When starved for nitrogen, diploid strains enter a pseudohyphal growth mode that depends on elements of the same MAPK cascade (5, 15). In comparison with wild-type diploid strain, *hsl7*Δ/*hsl7*Δ diploid strain exhibited enhanced pseudohyphal growth (Fig. 3*C*), but the *hsl7*Δ/*hsl7*Δ *ste20*Δ/*ste20*Δ strain did not form pseudohyphae (Fig. 3*C*). These findings strongly suggest that Hsl7p negatively regulates the MAPK-signaling pathway essential for filamentous growth by interacting with Ste20p. We then asked whether Hsl7p is involved in haploid mating, a process that requires components of the same MAPK cascade. We assayed the mating efficiencies and the activities of mating-specific reporter (*FUS1*-promoter-luciferase fusion) of wild-type and *hsl7*Δ haploid cells. We did not find any difference either in the mating efficiencies or in the luciferase activities between wild-type cells and *hsl7*Δ cells (data not shown). Therefore, Hsl7p does not appear to be involved in the MAPK-dependent signaling pathway during mating.

To confirm the possibility that Hsl7p negatively regulates MAPK cascade in filamentous growth-signaling pathway, we used the *STE12*-dependent transcriptional reporter (*FRE-lacZ*) (6). Because transcription from FREs, which contain the binding sites for Ste12 and Tec1p transcription factors (5, 38) (both factors were required for filamentous growth), is induced upon nitrogen starvation but not in response to mating pheromone (18, 28), *FRE-lacZ* reflects the activity of MAPK cascade during invasive growth and pseudohyphal development. Compared with the wild-type haploid strain, *FRE*-dependent transcription was induced about 1.5-fold in the

Table 1. Two-hybrid interactions among Ste20p, Cdc42p, and Hsl7p

Activating domain fusion	LexA DNA-binding domain fusion	Relative luciferase activity*
Ste20p (1–495)	Vector	1.0
Ste20p (1–495)	Cdc42p	18.6
Ste20p (1–495)	Hsl7p	7.4
Vector	Cdc42p	1.4
Vector	Hsl7p	1.5
Ste20p (1–495)	Hsl7p (with overexpression of *CDC42*)	1.7
Ste20p (1–495)	Cdc42p (with overexpression of *HSL7*)	3.1

*The relative luciferase activities are normalized to that for Ste20p-vector.

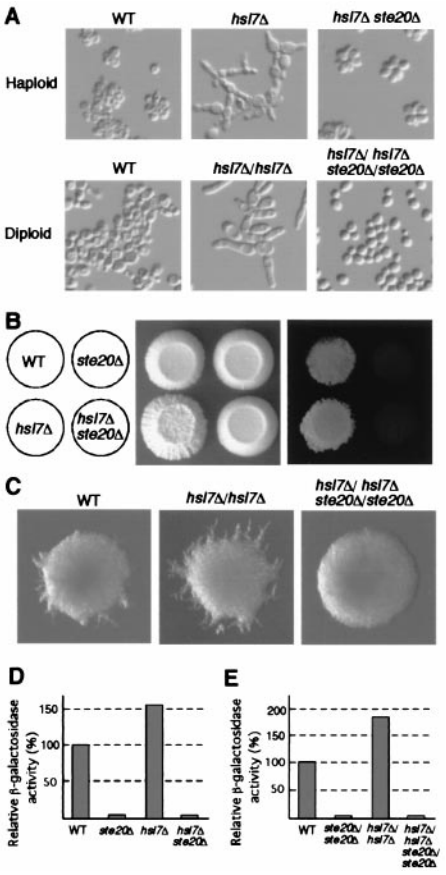

FIG. 3. Disruption of *HSL7* stimulates haploid invasive growth and diploid pseudohyphal development. (*A*) Elongated cell morphology of the haploid *hsl7*Δ and diploid *hsl7*Δ/*hsl7*Δ strains. Deletion of *STE20* abolished their elongated cell morphology. Yeast strains were cultured at 30°C in yeast extract/peptone/dextrose (YPD) medium for 3 days. Cells were visualized under the microscope with Nomarski optics. (*B*) Disruption of *HSL7*-stimulated invasive growth in haploid cells. (*Left*) Genotypes of the strains examined. (*Center*) Total growth. (*Right*) Haploid invasive growth. Σ1278b-derived strains: YAF1108 (*MAT***a** *HSL7*$^+$ STE20$^+$ leu2 ura3) and its otherwise isogenic derivatives YAF1191 (*MAT***a** *hsl7*Δ::*LEU2*), YAF1192 (*MAT***a** *ste20*Δ), and YAF1193 (*MAT***a** *hsl7*Δ::*LEU2 ste20*Δ). Strains were streaked onto YPD plates and grown for 3 days at 30°C. The plate shown in *Center* was rinsed under a stream of running water to distinguish surface growth from invasive growth by the degree of agar penetration (8). (*C*) Disruption of *HSL7* enhanced pseudohyphal growth in diploid cells. Diploid strain YAF1111 (*MAT***a**/*MATα HSL7*/*HSL7 STE20*/*STE20 leu2*/*leu2 ura3*/*ura3*) was constructed from YAF1108 and YAF1110 (*MATα HSL7*$^+$ *STE20*$^+$ *leu2 ura3*) in the Σ1278b background. Diploid strains YAF1194 (*MAT***a**/*MATα hsl7*Δ::*LEU2*/*hsl7*Δ::*LEU2*), YAF1195 (*MAT***a**/*MATα ste20*Δ/*ste20*Δ) and YAF1196 (*MAT***a**/*MATα hsl7*Δ::*LEU2*/*hsl7*Δ::*LEU2 ste20*Δ/*ste20*Δ) are YAF1111 derivatives. Every diploid strain contained vectors carrying *URA3* and/or *LEU2* to complement the *ura3* and/or *leu2* auxotrophies. These transformants were streaked on SLAD medium (15) and allowed to grow for 4 days. Resulting colonies were photographed. (*D* and *E*) Expression of the *FRE-lacZ* reporter gene. The eight strains described in *B* and *C* were transformed with a plasmid YEpU-FTyZ (6) (and a *LEU2*-containing vector to complement *leu2*), and β-galactosidase activity was measured. (*D*) Haploid strains on SD medium. (*E*) Diploid strains on nitrogen-starved medium. Activities were normalized to protein concentration and are shown as relative to the activities of wild-type strain. Values are the averages of measurements made in triplicate.

haploid *hsl7*Δ strain (Fig. 3*D*). Deletion of *STE20* in the *hsl7*Δ background eliminated *FRE*-dependent transcription (Fig. 3*D*). In the diploid *hsl7*Δ/*hsl7*Δ strain, *FRE-lacZ* expression was induced 1.8-fold on nitrogen-starved media (Fig. 3*E*) as compared with that of wild-type strain. Deletion of *STE20* also eliminated the *FRE-lacZ* activity in the *hsl7*Δ/*hsl7*Δ background (Fig. 3*E*). These data support the model that Hsl7p functions as a negative regulator of Ste20p in filamentous growth-signaling pathway.

Diploid *hsl7*Δ/*hsl7*Δ Strain Forms Pseudohyphae on Nitrogen-Rich Medium. We determined whether or not *hsl7*Δ/*hsl7*Δ diploid strain would form pseudohyphae on nitrogen-rich medium. In contrast to the wild-type diploid strain, *hsl7*Δ/*hsl7*Δ diploid strain showed pseudohyphal development after 2 weeks (Fig. 4). In addition, *FRE-lacZ* expression of disruptants also was induced 1.3-fold on nitrogen-rich medium relative to that of wild-type strain, indicating that the MAPK-dependent cascade is constitutively activated in *hsl7*Δ/*hsl7*Δ diploid cells.

Overexpression of Hsl7p Inhibits Diploid Pseudohyphal Growth. If binding of Hsl7p to Ste20p is essential for negative regulation of its activity, overexpression of *HSL7* may inhibit diploid pseudohyphal growth. To overproduce Hsl7p, we fused the *LEU2* promoter to the *HSL7* ORF on a multicopy vector (YEUp-HSL7Lp). Indeed, overexpression of *HSL7* in diploid strains inhibited pseudohyphal development (Fig. 5*A*).

Slight Overexpression of *CDC42* Reverses the Inhibitory Effect of *HSL7* Overexpression on Diploid Pseudohyphal Growth. The interaction between Cdc42p and Ste20p is essential for pseudohyphal development (19, 20). If both Hsl7p and Cdc42p bind to the same noncatalytic region of Ste20p, inhibition of pseudohyphal growth by *HSL7* overexpression will be reversed by the simultaneous overexpression of *CDC42*. Thus, we examined the effect of overexpression of *CDC42* on the inhibition of pseudohyphal development caused by the overexpression of *HSL7*. We found that slight overexpression of *CDC42* (*CDC42* on low-copy vector) eliminated the inhibitory effect of *HSL7* overexpression (Fig. 5*B*). We also found that *STE20* overexpression (*STE20* on high-copy vector) reverses the inhibitory effect of *HSL7* overexpression (Fig. 5*B*). These results suggested the possibility that Cdc42p competes with Hsl7p for Ste20p binding. We used the two-hybrid system to test this model. We cloned *CDC42* into the reporter plasmid, pLexAop-LucU, for overexpression from its native promoter (pLexAop-LucU-Cdc42p) and used this construct for two-hybrid analysis. Overexpression of Cdc42p resulted in a decrease in luciferase activity associated with the Ste20p-Hsl7p two-hybrid interaction (Table 1). Moreover, We cloned *HSL7* into pLexAop-LucU for *HSL7* overexpression (pLexAop-LucU-Hsl7p). Overexpression of Hsl7p also resulted in a decrease in luciferase activity associated with the Ste20p-Cdc42p two-hybrid interaction (Table 1). These results suggested that Cdc42p competes with Hsl7p for Ste20p binding to allow diploids to form pseudohyphae in response to nitrogen starvation.

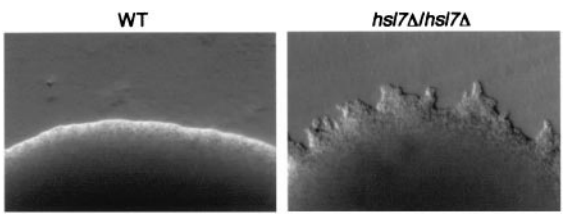

FIG. 4. Pseudohyphal growth of the *hsl7*Δ/*hsl7*Δ diploid strain on nitrogen-rich medium. Wild-type diploid (YAF1111) and *hsl7*Δ/*hsl7*Δ (YAF1194) strains containing a *URA3*-containing vector and/or a *LEU2*-containing vector to complement *ura3* and/or *leu2* were streaked on SLAD medium containing 5 mM ammonium sulfate and were incubated for 2 weeks at 30°C.

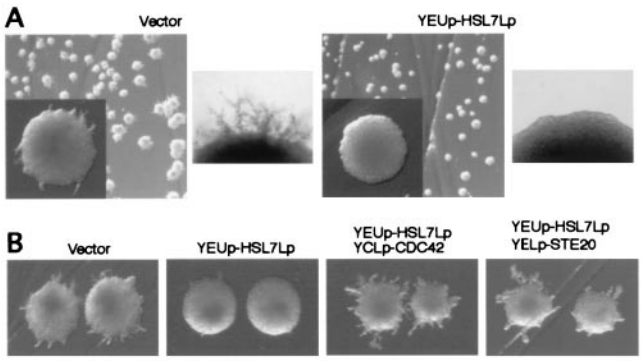

FIG. 5. (*A*) Overproduction of *HSL7* inhibits diploid pseudohyphal growth. Wild-type diploid strain YAF1111 containing a *LEU2*-vector (pRS315) was transformed with plasmids described at the top of the images. Cells of those strains were streaked on SLAD medium and incubated for 4 days at 30°C. (*Left*) Wild-type diploid cells containing vector, YEUp3. (*Right*) Wild-type diploid cells containing the plasmid for *HSL7* overproduction, YEUp-HSL7Lp. (*B*) Simultaneous expression of *CDC42* or *STE20* reversed the inhibitory effect to pseudohyphal development of *HSL7*-overexpressed cells. Strain YAF1111 was transformed with plasmids described at the top of the images. Cells of those strains were streaked on SLAD medium and incubated for 4 days at 30°C. YCLp-CDC42 is the *LEU2* plasmid for slight overproduction of *CDC42*; YELp-STE20 is the *LEU2* plasmid for overexpression of *STE20*.

DISCUSSION

We have described the characterization of yeast *HSL7*, which we identified from a screen for mutants exhibiting filamentous growth on rich medium. *HSL7* encodes a protein that is a member of a highly conserved protein family. One family member, the *S. pombe* Skb1p protein, had been identified from a two-hybrid screen for proteins that interact with *S. pombe* Shk1p (Ste20p/p65^{PAK} homologue) (33, 34). Based on binding assays and two-hybrid analyses, Hsl7p interacts with Ste20p, as suggested by the interaction *S. pombe* of Skb1p with Shk1p. *HSL7* disruption in haploid and diploid strains resulted in morphological changes (cell elongation) in both haploids and diploids, enhancement of invasive growth in haploids, enhancement of pseudohyphal growth on nitrogen starvation medium, and induction of pseudohyphal growth on nitrogen-rich medium in diploids. Moreover, all of these *hsl7* phenotypes were blocked by disruption of *STE20*. These facts can be explained by positing that Hsl7p inhibits Ste20p through their interaction (Fig. 6). This assumption was supported by the fact

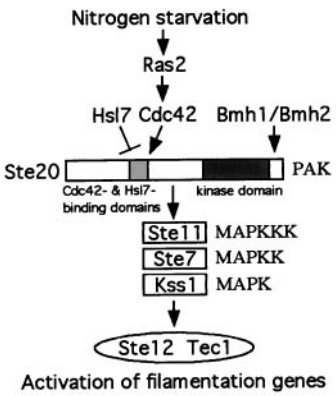

FIG. 6. Model for the role of Hsl7p during filamentous growth. Hsl7p binds to Ste20p to repress its activity. In response to nitrogen starvation, Ras2p activates Cdc42p and activated Cdc42p interferes with binding of Hsl7p to Ste20p. Two 14–3-3 proteins, Bmh1p and Bmh2p, which are essential for the pathway leading to pseudohyphal growth, also interact with the C terminus of Ste20p (37).

that overexpression of *HSL7* could inhibit pseudohyphal growth.

How is the activity of Ste20p regulated by Hsl7p in the filamentous growth-signaling pathway? One possible explanation is that the transcription of *HSL7* is regulated in response to nitrogen starvation. To test this possibility, we made a *HSL7* promoter–luciferase gene fusion to monitor the levels of *HSL7* expression in response to nitrogen starvation. However, we could not find any decrease in the measured luciferase activities (data not shown). Moreover, the transcript level of *HSL7* remained constant (data not shown), indicating that *HSL7* was constitutively expressed. We imagined another explanation based on the observation that both Cdc42p and Hsl7p bind to the N-terminal region of Ste20p. The identified Hsl7p-binding domain of Ste20p (amino acid 258–495) includes the Cdc42p-binding domain (amino acid 335–370), suggesting that Cdc42p and Hsl7p may bind to the same or neighboring regions of Ste20p. Although overexpression of *HSL7* inhibits pseudohyphal growth, slight overexpression of *CDC42* with overexpression of *HSL7* reverses pseudohyphal growth (Fig. 5*B*). Therefore, these findings suggest the possibility that Cdc42p may compete for binding to Ste20p with Hsl7p in response to nitrogen starvation (Fig. 6). Two-hybrid analysis of their interactions supported this idea. Recent work indicated that the interaction of Cdc42p to Ste20p is essential for pseudohyphal development (19, 20), but not for mating. Ste20p lacking the Cdc42p-binding region cannot localize properly (19, 20), causing a defect in pseudohyphal development. Overexpression of *HSL7*, which leads to inhibition of pseudohyphal growth, may interfere with the binding of Cdc42p to Ste20p. In this context there is a possibility that *HSL7* overexpression causes mislocalization of Ste20p. A detailed analysis of localization of Ste20p in *HSL7*-overexpressing cells may be necessary. In conclusion, Hsl7p may be a potent negative regulator of Ste20p in *S. cerevisiae* filamentous growth-signaling pathway. The identification of a novel Ste20p regulator will provide additional insights into the regulation of PAKs in both yeasts and higher organisms.

We thank J. Thorner, M. Lorentz, J. Heitman, J. Chant, K. Tanaka, C. Oka, Y. Arikawa, Y. Koyama, T. Murakami, W. E. Timberlake, C. J. Gimeno, C. A. Styles, J. R. Pringle, Y. Kikuchi, and G. R. Fink for generously providing yeast strains and plasmids. We also thank J. Chant and M. Ohara for the critical reading of the manuscript.

1. Bardwell, L., Cook, J. G., Inouye, C. J. & Thorner, J. (1994) *Dev. Biol.* **166,** 363–379.
2. Cobb, M. H. & Goldsmith, E. J. (1995) *J. Biol. Chem.* **270,** 14843–14846.
3. Denhardt, D. T. (1996) *Biochem. J.* **318,** 729–747.
4. Herskowitz, I. (1995) *Cell* **80,** 187–195.
5. Liu, H., Styles, C. A. & Fink, R. G. (1993) *Science* **262,** 1741–1744.
6. Cook, J. G., Bardwell, L. & Thorner, J. (1997) *Nature (London)* **390,** 85–88.
7. Madhani, H. D., Styles, C. A. & Fink, G. R. (1997) *Cell* **91,** 673–684.
8. Roberts, R. L. & Fink, G. R. (1994) *Genes Dev.* **8,** 2974–2985.
9. Zhou, Z., Gartner, A., Cade, R., Ammerer, G. & Errede, B. (1993) *Mol. Cell. Biol.* **13,** 2069–2080.
10. Polverino, A., Frost, J., Yang, P., Hutchison, M., Neiman, A. M., Cobb, M. H. & Marcus, S. (1995) *J. Biol. Chem.* **270,** 26067–26070.
11. Brown, J. L., Stowers, L., Baer, M., Trejo, J., Coughlin, S. & Chant, J. (1996) *Curr. Biol.* **6,** 598–605.
12. Frost, J. A., Xu, S., Hutchison, M. R., Marcus, S. & Cobb, M. H. (1996) *Mol. Cell. Biol.* **16,** 3707–3713.
13. Bagrodia, S., Derijard, B., Davis, R. J. & Celione, R. A. (1995) *J. Biol. Chem.* **270,** 27995–27998.
14. Leberer, E., Dignard, D., Harcus, D., Thomas, D. Y. & Whiteway, M. (1992) *EMBO J.* **11,** 4815–4824.
15. Gimeno, C. J., Ljungdahl, P. O., Styles, C. A. & Fink, G. R. (1992) *Cell* **68,** 1077–1090.
16. Simon, M. N., De Virgilio, C., Souza, B., Pringle, J. R., Abo, A. & Reed, S. I. (1995) *Nature (London)* **376,** 702–705.
17. Zao, Z. S., Leung, T., Manser, T. & Lim, L. (1995) *Mol. Cell. Biol.* **15,** 5246–5257.
18. Mosch, H.-U., Roberts, R. L. & Fink, G. R. (1996) *Proc. Natl. Acad. Sci. USA* **93,** 5352–5356.
19. Peter, M., Neiman, A. M., Park, H.-O., Lohuizen, M. & Herskowitz, I. (1996) *EMBO J.* **15,** 7046–7059.
20. Leberer, E., Wu, C., Leeuw, T., Fourest-Lieuvin, A., Segal, J. E. & Thomas, D. Y. (1997) *EMBO J.* **16,** 83–97.
21. Sherman, F., Fink, G. R. & Hicks, J. B. (1986) *Methods in Yeast Genetics* (Cold Spring Harbor Lab. Press, Plainview, NY).
22. Rothstein, R. J. (1983) *Methods Enzymol.* **101,** 202–211.
23. Guldener, U., Heck, S., Fielder, T., Beinhauer, J. & Hegemann, J. H. (1996) *Nucleic Acids Res.* **24,** 2519–2524.
24. Burns, N., Grimwade, B., Ross-Macdonald, P. B., Choi, E.-Y., Finberg, K., Roederm, G. S. & Snyder, M. (1994) *Genes Dev.* **8,** 1087–1105.
25. Altschul, S. F., Gish, W., Miller, W., Meyers, E. W. & Lipman, D. J. (1990) *J. Mol. Biol.* **215,** 403–410.
26. Sikorski, R. S. & Hieter, P. (1989) *Genetics* **122,** 19–27.
27. Wu, C., Whiteway, M., Thomas, D. Y. & Leberer, E. (1995) *J. Biol. Chem.* **270,** 15984–15992.
28. Madhani, H. D. & Fink, G. R. (1997) *Science* **275,** 1314–1317.
29. Butler, G. & Thiele, D. J. (1991) *Mol. Cell. Biol.* **11,** 476–485.
30. Fujita, A., Oka, C., Arikawa, Y., Katagai, T., Tonouchi, A., Kuhara, S. & Misumi, Y. (1994) *Nature (London)* **372,** 567–570.
31. Ma, X., Lu, Q. & Grunstein, M. (1996) *Genes Dev.* **10,** 1327–1340.
32. Wilson, R., Ainscough, R., Anderson, K., Baynes, C., Berks, M., Bonifield, J., Burton, J., Connell, M., Copsey, T., Cooper, J., *et al.* (1994) *Nature (London)* **368,** 32–38.
33. Gilbreth, M., Yang, P., Wang, D., Frost, J., Polverino, A., Cobb, M. H. & Marcus, S. (1996) *Proc. Natl. Acad. Sci. USA* **93,** 13802–13807.
34. Marcus, S., Polverino, A., Chang, E., Robbins, D., Cobb, M. H. & Wigler, M. H. (1995) *Proc. Natl. Acad. Sci. USA* **92,** 6180–6184.
35. Manser, E., Leung, T., Salihuddin, H., Zao, Z. S. & Lim, L. (1994) *Nature (London)* **367,** 40–46.
36. Kron, S. J., Styles, C. A. & Fink, G. R. (1994) *Mol. Biol. Cell* **5,** 1003–1022.
37. Roberts, R. L., Mosch, H.-U. & Fink, G. R. (1997) *Cell* **89,** 1055–1065.
38. Gavrias, V., Andrianopoulos, A., Gimeno, C. J. & Timberlake, W. E. (1996) *Mol. Microbiol.* **19,** 1255–1263.
39. Laemmli, U. K. (1970) *Nature (London)* **227,** 680–685.